Preferential Fluid Flow in the Human Trabecular Meshwork Near Collector Channels

Cheryl R. Hann and Michael P. Fautsch

Purpose. To determine whether preferential pathways exist within the human trabecular meshwork, pigmented and nonpigmented regions adjacent to and between collector channels were examined, and the configuration of the juxtacanalicular tissue (JCT) was analyzed.

Methods. Healthy whole human eyes were perfused at 10 or 25 mm Hg with 0.5 μm fluorescent beads. Tissue wedges of pigmented and nonpigmented meshwork (with and without collector channels) were dissected from each eye and examined by confocal microscopy. Bead concentration adjacent to and between collector channels was quantified. The configuration of the JCT adjacent to collector channels from whole eyes perfused at 20 mm Hg was analyzed by light microscopy.

Results. Eyes perfused at 25 mm Hg had more beads adjacent to collector channels in pigmented than in nonpigmented regions (4.9% ± 3.5% vs. 1.1% ± 0.9%; $P = 0.02$). In pigmented regions without collector channels, bead concentration was decreased by fivefold (4.9% ± 3.5% vs. 0.96% ± 0.88%; $P = 0.04$). Perfusion at 25 mm Hg increased beads by threefold under pigmented collector channels compared with the same regions in eyes perfused at 10 mm Hg. Expansion of the JCT occurred more often under collector channels at 25 mm Hg than at 10 mm Hg (44% vs. 17%; $P = 0.01$). The JCT region under collector channels was expanded compared with JCT regions between adjacent collector channels (1053 ± 424 μm^2 vs. 571 ± 216 μm^2; $P < 0.001$).

Conclusions. Increased levels of beads in pigmented trabecular meshwork adjacent to collector channels suggest preferential flow pathways are present in human trabecular meshwork. At elevated pressure, the JCT region under collector channels is expanded, possibly because of increased fluid flow. (*Invest Ophthalmol Vis Sci.* 2009;50:1692–1697) DOI:10.1167/iovs.08-2375

The route of aqueous humor drainage from the human anterior segment occurs primarily through the trabecular meshwork. From the trabecular meshwork, aqueous humor drains into Schlemm's canal and empties into collector channels that lead to the episcleral venous system. Although the morphology of the trabecular meshwork and Schlemm's canal appear similar around the circumference of the eye, studies with various tracers have shown that fluid flow is not equal within the trabecular meshwork and that preferential pathways or flow to areas of lower resistance exist in the trabecular meshwork.[1–8] Perfusion with cationic ferritin resulted in segmental labeling in monkey eyes,[5] in healthy human eyes,[6,7] and in human glaucoma eyes.[8]

Pigmented and nonpigmented regions of the trabecular meshwork observed during gonioscopic examination were the first clinical evidence that suggested preferential fluid flow routes might be present in the trabecular meshwork. Analysis of pigmented regions found these regions correlated with the presence of collector channels in human eyes (Tanchel NA, et al. *IOVS* 1984;25:ARVO Abstract 7). Giant vacuoles, pressure-sensitive structures found in the endothelium of Schlemm's canal, were also more prevalent near collector channels, indicating an increased fluid flow rate.[9] Accumulation of fluorescent beads near collector channels in bovine eyes after perfusion at normal and elevated pressure suggests that preferential flow through the trabecular meshwork is not restricted to human eyes.[10] In the same study, expanded areas of the juxtacanalicular tissue (JCT) adjacent to the collector channels were also observed in bovine eyes at elevated pressure.

Expanded JCT regions were compared with Pacchionian bodies, protrusions of the arachnoid through the dura.[11] These expanded regions were subsequently called Pacchionian-like bodies[12] or proliferations of the inner wall endothelial cells in human eyes[13] and hernias[14] or protrusions in monkey eyes.[15] In these regions, the inner wall of Schlemm's canal protrudes into the canal in a hillock-like formation, and the overlying endothelium balloons and appears to lose close contact with the underlying JCT tissue. Expanded JCT has been observed in healthy monkey eyes and human glaucomatous eyes after laser treatment.[5,16,17] Perfusion with cationic ferritin indicated the expanded JCT regions were a route of preferential fluid flow.[5,17]

Preferential fluid flow may occur where collector channels are more prevalent and where the fluid exits the anterior chamber, in areas of pressure change, or where the extracellular matrix is altered or absent. In this study, we examined fluid flow in pigmented and nonpigmented regions within human trabecular meshwork, the association between these regions and collector channels, and the configuration of the JCT adjacent to and between collector channels.

Materials and Methods

Preferential Fluid Flow Studies

Whole Eye Perfusion. Four pairs of whole healthy human eyes with pigmented irises (mean age, 72 ± 16 years) were obtained from the Minnesota Lion's Eye Bank within 12 hours of death (mean time, 8.8 ± 3.5 hours; range, 4–12 hours). All procedures concerning the use of human tissue were in accordance with the Declaration of Helsinki and Mayo Clinic Institutional Review Board. One eye of each pair was perfused at 10 mm Hg ($n = 4$), and the fellow eye was perfused at 25 mm Hg ($n = 4$) with Dulbecco's modified Eagle's medium (DMEM; Mediatech, Herndon, VA) for 30 minutes to establish fluid flow through the meshwork. Anterior chamber exchange using a 1-mL volume of DMEM containing 0.002% carboxylate-modified microspheres (0.5 μm; FluoSpheres; Molecular Probes, Eugene, OR) was performed. Eyes were continuously perfused for an additional 30

From the Department of Ophthalmology, Mayo Clinic, Rochester, Minnesota.

Supported in part by National Institutes of Health Research Grants EY 07065 and EY 15736; Research to Prevent Blindness, Inc., New York, NY; and the Mayo Foundation, Rochester, MN.

Submitted for publication June 3, 2008; revised October 7 and November 18, 2008; accepted February 26, 2009.

Disclosure: **C.R. Hann**, None; **M.P. Fautsch**, None

The publication costs of this article were defrayed in part by page charge payment. This article must therefore be marked "*advertisement*" in accordance with 18 U.S.C. §1734 solely to indicate this fact.

Corresponding author: Michael P. Fautsch, Department of Ophthalmology, Mayo Clinic, 200 First Street SW, Rochester, MN 55905; fautsch.michael@mayo.edu.

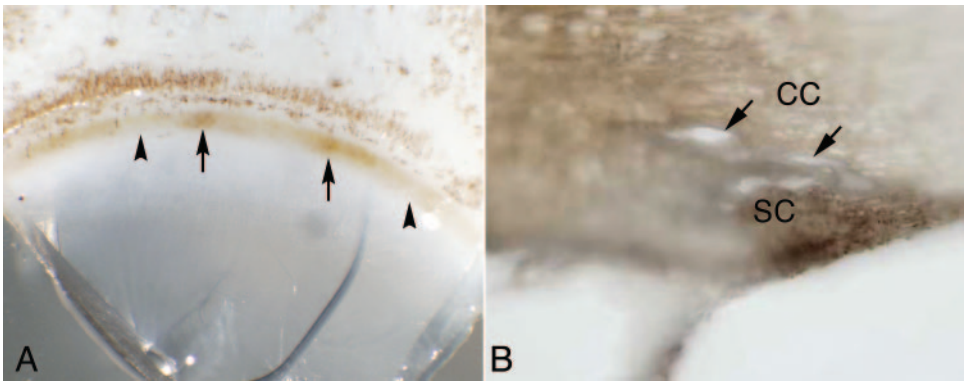

FIGURE 1. Dissection of trabecular meshwork (TM) demonstrating pigmentation and collector channels. (**A**) Tissue wedge of human anterior segment showing variable pigmentation in the trabecular meshwork. *Arrows*: pigmented areas; *arrowheads*: nonpigmented areas. (**B**) Tissue wedge of trabecular meshwork with collector channel (CC) extending from the central region of Schlemm's canal (SC), in characteristic stovepipe formation, into the sclera (*arrows*).

minutes with DMEM containing 0.002% beads. After perfusion, anterior chamber exchange was performed with 4% paraformaldehyde in 0.1 M phosphate buffer followed by continuous perfusion with fixative for 30 minutes. Perfusion was stopped, and anterior segments were dissected from the whole globes and immersed in the same fixative.

Trabecular Meshwork Dissection and Confocal Microscopy. The lens, iris, and ciliary body were removed from the anterior segment. The eye was divided into quadrants. Trabecular meshwork (1–3 mm wedges) containing pigmented or nonpigmented regions from two quadrants were dissected from each eye (Fig. 1A). Radial sections were made until a collector channel could be visualized under a dissecting scope (Fig. 1B). In addition, wedges without collector channels were collected from pigmented and nonpigmented regions. Wedges were stained for 30 minutes in DiI (50 μg/mL in PBS; Molecular Probes) according to the method of Honig and Hume.[18] After staining, wedges were rinsed with PBS and mounted (CultureWells; Grace Biolabs, Bend, OR) with anti-fade medium (Vectashield; Vector Laboratories, Burlingame, CA) containing DAPI. The wells were coverslipped with cover glasses (Gold Seal no. 1.5; Electron Microscopy Sciences, Fort Washington, PA). Mounted wedges were examined on a confocal laser microscope (Zeiss 510; Carl Zeiss, Thornwood, NY).

Data Retrieval and Analysis. Volumes of each wedge were collected (mean volume size, 15 μm) and analyzed with image processing software (Zeiss KS 400; Carl Zeiss). A macro was written to automate analysis of the trabecular meshwork and collector channel regions. DiI stained the cell cytoplasm and beams red, DAPI labeled the nuclei blue, and fluorescent beads appeared green. To quantitate the beads per total area, the trabecular meshwork area was traced using the inner wall of Schlemm's canal and the outer uveal meshwork as boundaries. After tracing, the total area was calculated (Fig. 2A). With the green channel on the software program, the total area of beads was calculated within the trabecular meshwork (Fig. 2B) and expressed as a percentage of the total trabecular meshwork area. The diameter of the collector channel orifice was measured interactively in wedges with collector channel orifices. The program selected the center point of the orifice measurement and added an area measuring 10 μm on either side of the center point (for a total of 20 μm). This orifice measurement was used to delineate the area of the trabecular meshwork directly under the collector channel (Fig. 2C). Two areas anterior to the collector channel (each measuring 20 μm) and two areas posterior to the collector channel (also measuring 20 μm) were analyzed. Anterior areas were designated A1 and A2, whereas the posterior areas were designated P1 and P2 (Fig. 2C). Using the program's green channel, the total area of beads was measured in each of these regions and was calculated as a percentage of the total bead area (Fig. 2B). In wedges without collector channels, a sham orifice 30 μm long was drawn in the center of Schlemm's canal. Analysis then proceeded as described, with all regions designated in the same fashion.

Morphometric Analysis of JCT Configuration

Whole Eye Perfusion. Six healthy human eyes (donor age, 65.3 ± 9.5 years) were obtained from the Minnesota Lion's Eye Bank within 24 hours of donor death (mean time, 13.3 ± 7.7 hours; range, 5–23 hours). Whole eyes were perfused with Dulbecco's phosphate buffered-saline (Sigma, St. Louis, MO) containing 5.5 mM glucose at 20

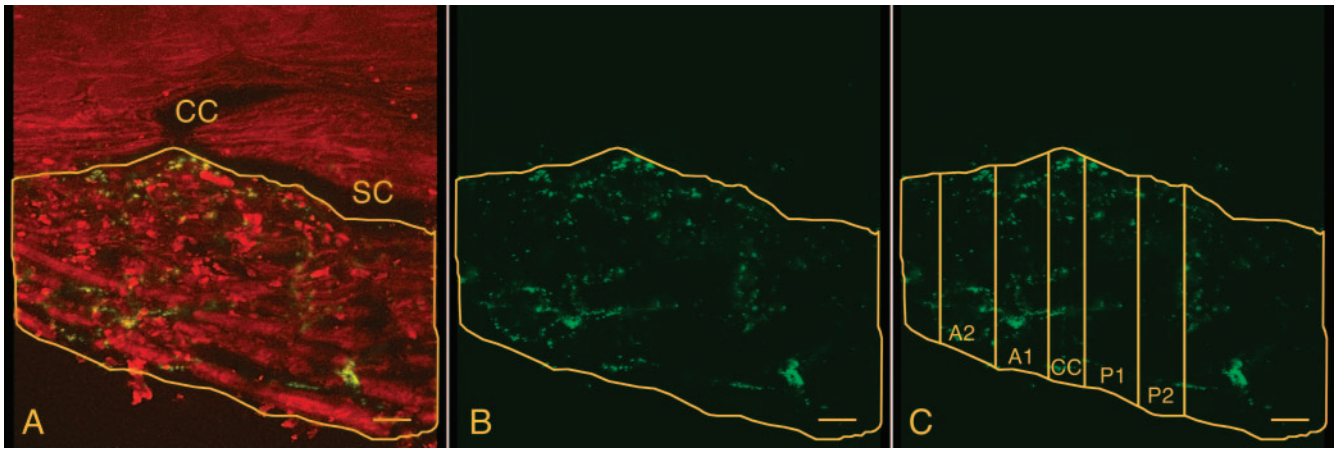

FIGURE 2. Calculation of bead area with the use of imaging software. (**A**) Total area of the trabecular meshwork was obtained by tracing the inner wall of Schlemm's canal (SC) and the uveal beams as boundaries (*yellow*). (**B**) Total area of the fluorescent beads (*green channel*) was calculated within the total trabecular meshwork area (*yellow outline*). (**C**) Regions analyzed included those directly under the collector channel (CC) orifice, those anterior to CC (A1, A2), and those posterior to CC (P1, P2). The bead area in each of these regions was computed as the percentage of total bead area (**B**, *green area*). Scale bar, 20 μm.

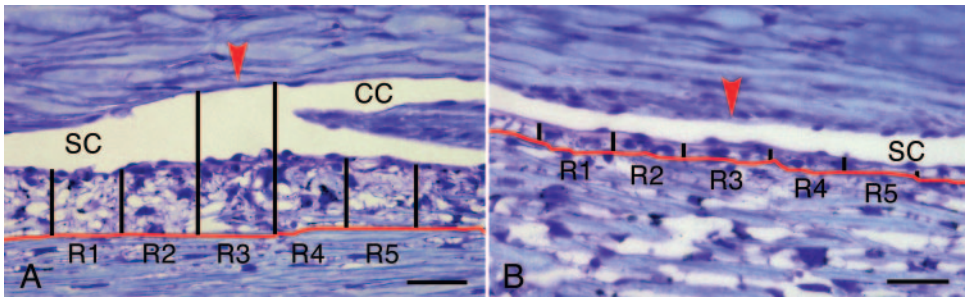

FIGURE 3. Analysis of JCT regions under and between collector channels using frontal sections. Images of the expanded JCT region under (**A**) and between (**B**) collector channels. JCT demarcation is traced in *red*. *Red arrowheads*: center of collector channel orifice (**A**) and center of analyzed region (**B**). Area of five consecutive 50-μm regions (R1–R5) was analyzed for area. SC, Schlemm's canal; CC, collector channel. Scale bar, 20 μm.

mm Hg for 2 hours. Eyes were perfusion fixed with 4% paraformaldehyde/2% glutaraldehyde in 0.1 M cacodylate buffer (pH 7.4) overnight. Eyes were divided into quadrants, and representative tissue wedges from each quadrant were processed in an ascending alcohol series and embedded in JB-4. Blocks were serially sectioned in a frontal orientation at 5 μm. Slides were stained with toluidine blue and examined by light microscopy.

Data Retrieval and Analysis. Sections from all six eyes were prescreened to select one block from each specimen that contained two collector channels. For each pair of collector channels to be analyzed, serial sections containing the collector channel orifices were counted and divided by 2. The central section was captured by digital imaging on a light microscope using 400× magnification. A "control" region from each specimen was selected equidistant between the collector channel orifices and was captured digitally. With the use of image processing software (KS 400; Carl Zeiss) and a custom analysis macro, the distance across the collector channel ostia was measured, and a center point was located in the ostia. Areas encompassing 125 μm to the right and left of the center point were calculated. The inner wall of Schlemm's canal and the JCT was traced on all digital images between the left and right marks. We used the image processing software (KS 400; Carl Zeiss) with a custom analysis macro to calculate the area within the 250-μm region underlying the collector channels. This area was further subdivided into 50-μm regions: region 1, 75 to 125 μm to the left of center point; region 2, 25 to 75 μm to the left of center point; region 3, 25 μm on either side of center point (collector channel orifice); region 4, 25 to 75 μm to the right of center point; region 5, 75 to 125 μm to the right of center point (Fig. 3A). Similar measurements were made for the control sections using the center of the length of Schlemm's canal as a starting point because no collector channel was present (Fig. 3B).

Statistical Analysis

A paired *t*-test was performed to determine whether there was a significant difference between JCT areas under collector channels (n = 12) and control regions (n = 6). In addition, *t*-tests were performed to determine differences in JCT area among the four regions adjacent to collector channel ostia (region 1 vs. regions 2–5). The five regions were compared within the collector channels with one-factor repeated-measures analysis of variance. Paired *t*-tests were used to compare the parameters within the five areas. An unpaired *t*-test was used to determine whether bead concentrations differed among the areas under or between collector channels in pigmented regions.

Qualitative Analysis of Expanded JCT Region

All confocal volumes of 10 and 25 mm Hg eyes were screened for the presence or absence of expanded JCT regions. The location of these regions was recorded to be either directly under the collector channel or between the collector channels. For a JCT region to be considered expanded, the region in question had to be (1) two or more times the height of the adjacent JCT, and (2) Schlemm's canal cells had to appear vacuolated and to be stacked on top of one another and lifting from the underlying extracellular matrix. In regions identified as expanded JCT, the green channel was examined to determine whether beads were found only in those areas.

RESULTS

Pigmented versus Nonpigmented Trabecular Meshwork

Pigmented and nonpigmented regions of trabecular meshwork adjacent to and between collector channels from eyes perfused with beads at 10 and 25 mm Hg were compared. In eyes perfused at 25 mm Hg, pigmented areas of the meshwork had more beads per area than nonpigmented regions (25 mm Hg: 4.9% ± 3.5% vs. 1.1% ± 0.9%; P = 0.02; Fig. 4A). Bead concentration was increased under collector channels compared with bead levels in areas between collector channels in pigmented regions (4.9% ± 3.5% vs. 0.96% ± 0.88%: P = 0.04). No statistical change was found in bead amounts between nonpigmented regions under or between collector channels (1.1% ± 0.9% vs. 1.6% ± 2.1%; P = 0.59).

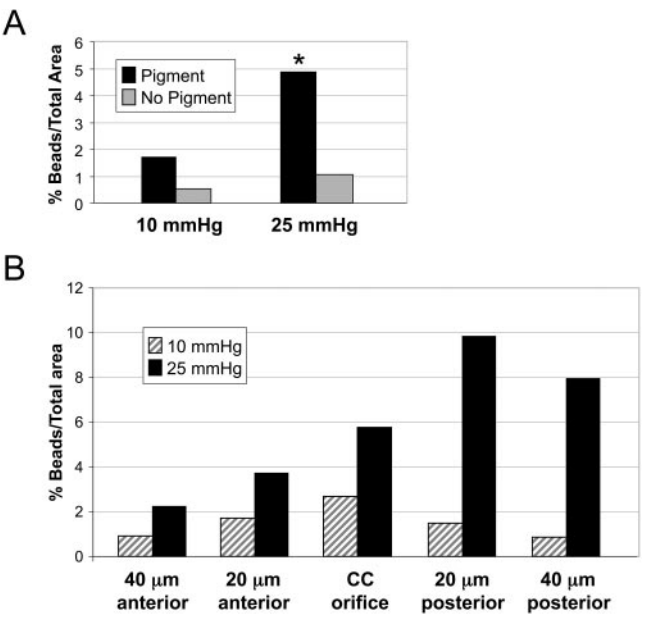

FIGURE 4. Comparison of bead density in pigmented and nonpigmented regions of trabecular meshwork. (**A**) Pigmented regions adjacent to collector channel had higher concentrations of beads than nonpigmented regions in the 10- and 25-mm Hg eyes. *P = 0.02. (**B**) In 10-mm Hg eyes, the collector channel orifice region had more beads than regions 20 and 40 μm away from the orifice. In the 25-mm Hg, anterior regions moving away from the collector channel orifice contained fewer beads. However, posterior regions contained more beads than the collector channel orifice.

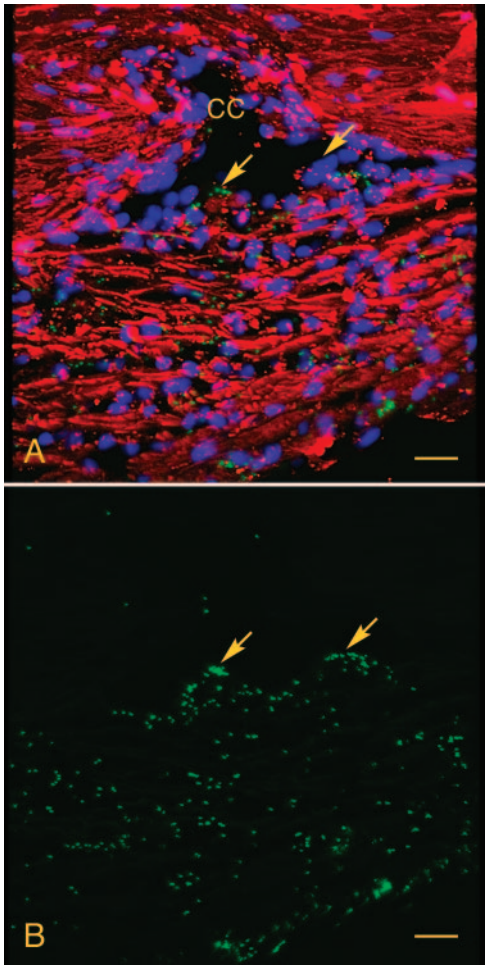

FIGURE 5. Distribution of beads within expanded JCT regions under collector channels. (**A**) Confocal volume showing expanded JCT area (*arrows*) under collector channel (CC) orifice. (**B**) *Green* channel of confocal image shown in (**A**). Fluorescent beads migrated to expanded JCT regions but did not localize to them. *Arrows*: expanded areas of JCT. Scale bar, 20 μm.

Comparison of eyes perfused at 25 mm Hg and 10 mm Hg showed collector channel orifices in eyes perfused at 25 mm Hg had a threefold increase of beads compared with similar regions in eyes perfused at 10 mm Hg. In 10-mm Hg eyes, bead numbers decreased with distance from the ostia in anterior and posterior regions (Fig. 4B). However, in 25-mm Hg eyes, beads were increased posteriorly to the collector channel ostia and decreased anteriorly (Fig. 4B). Percentages of beads per area in the 25-mm Hg eyes were greater than in anterior and posterior regions compared with 10-mm Hg perfused eyes.

Identification of Expanded JCT

Expanded JCT regions had a foamy appearance because of the expansion of Schlemm's canal cells and the underlying JCT region. Analysis of 16 tissue wedges from eyes perfused at 25 mm Hg identified seven expanded JCT regions associated with collector channels, whereas only two expanded JCT regions were identified in 12 wedges analyzed from eyes perfused at 10 mm Hg (44% vs. 17%; $P = 0.01$; Fig. 5A). No expanded JCT regions were found between collector channels in the 25-mm Hg or the 10-mm Hg perfused eyes ($n = 12$ tissue wedges for each perfusion pressure). Beads were found scattered within expanded JCT regions but were not specifically localized to these regions (Fig. 5B).

Analysis of Expanded JCT

Expansion of the JCT was found in association with collector channels in eyes perfused at 10 mm Hg and 25 mm Hg. Total JCT area under the collector channels (250 μm area) was significantly larger than a similarly sized control region between adjacent collector channels (1053 ± 424 μm^2 vs. 571 ± 216 μm^2; $P < 0.001$; Fig. 6). Expansion of the JCT region continued beyond the 125-μm area analyzed on either side of the collector channel ostia. No significant difference was found in expanded areas directly under collector channel ostia (region 3) compared with expanded regions on either side (regions 1, 2, 4, and 5).

DISCUSSION

This study confirmed that regions of the human trabecular meshwork under collector channels have a preference for increased fluid flow. Although other studies using tracers have found segmental labeling in the human and animal trabecular meshwork,[4–8,10] this is the first study analyzing preferential fluid flow in the JCT adjacent to collector channels in human eyes. Native biological pigment and tracer molecules move to these regions first. In eyes perfused at normal and elevated pressure, a larger number of fluorescent beads were found adjacent to collector channel ostia in regions of pigmentation. Decreased numbers of beads were found in areas without collector channels. The total JCT area under collector channels was found to be expanded nearly twofold compared with JCT

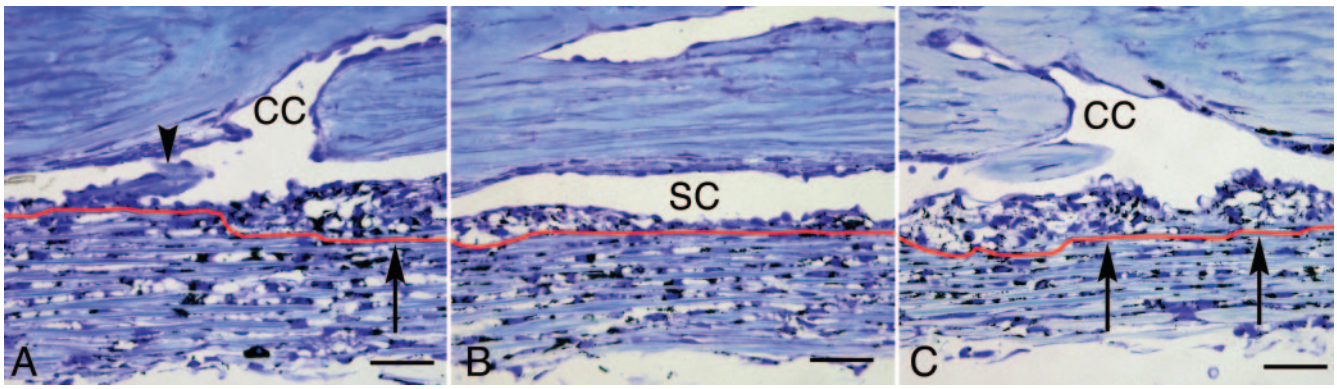

FIGURE 6. Expanded JCT adjacent to and between collector channels. (**A–C**, *red line*) JCT boundaries. (**A**) Collector channel orifice with expanded region on the right side of the micrograph (*black arrow*). *Arrowhead*: septum. (**B**) Region between collector channels showing minimal expansion of the JCT. (**C**) Expanded JCT under collector channel orifice (*black arrows*). CC, collector channel; SC, Schlemm's canal. Scale bars, 50 μm.

regions between collector channels. These results change our perception of how the human trabecular meshwork functions. Instead of fluid flow occurring homogeneously throughout the circumference of the meshwork, regions of preferential flow exist in areas adjacent to collector channels where fluid exits the anterior chamber.

Although preferential fluid flow occurs under collector channels, collector channels from pigmented and nonpigmented regions appear to function at different rates. One explanation may be that collector channel distribution is not uniform. Early studies suggested that collector channel placement around the circumference of the eye was irregular and had a tendency for increased collector channels in the inferior quadrant.[19] If more collector channels are located in the inferior quadrant, then presumably more fluid flow will occur in this region and more pigment will be accumulated. We also noted the presence of pigment more often in the nasal and inferior regions. Although this might have occurred because of the influence of gravity, where heavier pigment granules may accumulate, we do not believe this to be the case. Our eyes were perfused in the supine position, with the cornea facing up, yet in areas of pigmentation we still found increased bead accumulation.

Differences in collector channel flow may occur because some collector channels reside near larger episcleral venules, the final destination of aqueous. In a study of primate anterior sclera, Selbach et al.[20] found episcleral venules have a thick, innervated muscle wall. Innervated venules may influence episcleral venous pressure and, in turn, outflow facility and volume regulation.

In addition to collector channel number and location, several factors may explain the increased fluid flow in the trabecular meshwork region under collector channels. For fluid to flow from the trabecular meshwork into Schlemm's canal, a pressure difference must exist. The pressure differential between the trabecular meshwork and Schlemm's canal is 2 to 3 mm Hg.[21] Areas under collector channels, however, have a greater pressure differential which may increase to 6 mm Hg.[21] The increased pressure differential under collector channels allows for less resistance to fluid flow, enabling a more direct pathway for fluid to flow from the trabecular meshwork to collector channels. Expanded JCT may represent the normal morphology because of the greater pressure differential within this area. Whether the expanded JCT region or the pressure differential under collector channels is responsible for preferential fluid flow has not been determined.

Although the pressure differential may contribute to increased flow, drainage accessibility also undoubtedly plays a role. Collector channel ostial regions are the shortest and most efficient routes for aqueous to leave the anterior chamber. Aqueous flowing from the uveal meshwork to the ostia has a shorter route to travel than fluid that enters between two collector channels and must travel laterally to reach the collector channel ostia. The observation that bead numbers decrease with distance from the ostia and in regions between collector channels lends credence to this supposition.

One factor contributing to preferential flow may be changes in extracellular matrix interactions with Schlemm's canal cells in collector channel regions. Alterations in the extracellular matrix may change the dynamics of cell attachment, enabling JCT expansion and less fluid flow resistance. Preliminary examination of the expanded JCT regions by light and electron microscopy revealed a paucity of basement membrane material under ballooned Schlemm's canal endothelial cells. In healthy human eyes, a system of connecting fibrils described by Rohen et al.[22] anchors the Schlemm's canal endothelial cells to the basement membrane. Recent morphometric studies of these fibers found they were more prevalent in human eyes than in the eyes of species with washout.[23] Our laboratory found these fibers changed to a more elongated configuration under elevated pressure (Hann CR, et al. *IOVS* 2008;49:ARVO E-Abstract 1604). Further studies are warranted to determine whether anatomic differences are present in the expanded JCT regions in the connecting fibrils and their associated molecules under and between collector channels.

Expanded JCT regions appear to be pressure-sensitive structures that form more readily at higher pressures and provide increased flow area for aqueous humor.[5,16,17] Although expanded JCT regions were identified in eyes perfused at normal pressure, expanded JCT regions were significantly increased in eyes perfused at elevated pressure (44% vs. 17%; $P = 0.01$). Expanded JCT regions may form more readily at collector channels because of the lack of an outer wall in this area. Under elevated pressure, this effectively allows the inner wall to expand more freely, enabling the release of fluid. We found that collector channels have a sphere of influence as their adjacent regions of dilated JCT extend at least 100 μm on either side of the collector channel ostia. These areas were dilated to the same extent as the regions directly under the orifice.

Expansion of JCT regions under collector channels may cause loss of the funneling effect, as described by Johnson et al.[24] The funneling effect describes the fluid path of aqueous through the JCT in the region of inner wall pores such that the aqueous is directed, or funneled, preferentially to the pore. These specific flow regions adjacent to the pores reduce the overall JCT filtration area and increase the resistance within this tissue. Scott et al.,[23] in their comparative study of washout, noted in human eyes that connections between the inner wall and the JCT oppose the hydrodynamic forces and maintain outflow resistance. When this connection is absent or attenuated, as in bovine eyes, outflow facility will increase. Although this loss of the funneling effect may occur in expanded regions focally because of loss of contact between Schlemm's canal cells and the extracellular matrix, funneling may still occur in regions without expansion.

In this study, confocal images of radial sections and light microscopy images of frontal sections were used as independent methods to examine the JCT regions adjacent to collector channels. Direct comparisons of JCT size could not be made between confocal wedges and plastic sections. Although confocal imaging of radial sections has the advantage of being unprocessed and, therefore, not subject to shrinkage and heat, limitations exist, particularly by the small volume size (15 μm) and the inability to clearly delineate the JCT region. This sample size was good for the quantitation of beads under the collector channel, but it was difficult to determine the exact location of the 15-μm subvolume within the context of the complete collector channel volume. In subsequent work with vibratome sections, we found the complete collector channel volume, including the orifice, to be approximately 100 μm (Hann CR, Fautsch MP, unpublished observations, 2007). Light microscopy imaging of frontal sections enabled us to analyze several collector channels at once, view the tissue between adjacent collector channels, and study images coming in and going out of the orifices. Confocal and light microscopy imaging was important for verifying features related to increased fluid flow and expanded JCT regions.

In summary, we have identified regions under collector channels as areas of preferential fluid flow through the trabecular meshwork. These regions contain expanded JCT theoretically enabling less resistance to fluid flow. These studies suggest the eye may have an organ reserve[25] similar to kidney or liver in which only a portion of the collector channels are needed to maintain normal aqueous flow from the anterior chamber. As collector channels become altered with age or disease, other collector channels are available to assume the

functional burden. Further examination of the functional distribution of collector channels and the molecular analysis of the expanded JCT regions will be important for understanding how these areas preferentially move fluid through the trabecular meshwork.

Acknowledgments

The authors thank the late Douglas Johnson, MD, for initiating some of the ideas and experimental design presented in this manuscript.

References

1. Karg SJ, Garron LK, Feeney ML, McEwen WK. Perfusion of human eyes with latex microspheres. *Arch Ophthalmol.* 1959;61:68–71.
2. Inomata H, Bill A, Smelser GK. Aqueous humor pathways through the trabecular meshwork and into Schlemm's canal in the cynomolgus monkey (*Macaca irus*). *Am J Ophthalmol.* 1972;73:760–789.
3. Tripathi RC. Mechanism of the aqueous outflow across the trabecular wall of Schlemm's canal. *Exp Eye Res.* 1971;11:116–121.
4. Sabanay I, Gabelt BT, Tian B, Kaufman PL, Geiger B. H7 effects on the structure and fluid conductance of monkey trabecular meshwork. *Arch Ophthalmol.* 2000;118:955–962.
5. Melamed S, Epstein DL. Alterations of aqueous humour outflow following argon laser trabeculoplasty in monkeys. *Br J Ophthalmol.* 1987;71:776–781.
6. Ethier RC, Chan DWH. Cationic ferritin changes outflow facility in human eyes whereas anionic ferritin does not. *Invest Ophthalmol Vis Sci.* 2001;42:1795–1802.
7. Hann CR, Bahler CK, Johnson DH. Cationic ferritin and segmental flow through the trabecular meshwork. *Invest Ophthalmol Vis Sci.* 2005;46:1–7.
8. de Kater AW, Melamed S, Epstein DL. Patterns of aqueous humor outflow in glaucomatous and nonglaucomatous human eyes: a tracer study using cationized ferritin. *Arch Ophthalmol.* 1989;107:572–576.
9. Parc CE, Johnson DJ, Brilakis HS. Giant vacuoles are found preferentially near collector channels. *Invest Ophthalmol Vis Sci.* 2000;41:2984–2990.
10. Battista SA, Lu Z, Hofmann S, Freddo TF, Overby D, Gong H. Reduction of the available area for aqueous humor outflow and increase in meshwork herniations into collector channels following acute IOP elevation in bovine eyes. *Invest Ophthalmol Vis Sci.* 2008;49:5346–5352.
11. Wegefarth P. Studies on cerebro-spinal fluid, V: the drainage of intra-ocular fluids. *J Med Res Boston* 1914–1915;31:119–147.
12. Wolf E. Pacchionian-like bodies in the human canal of Schlemm. *Br J Ophthalmol.* 1952;36:100–103.
13. Rohen JW. Morphology and pathology of the trabecular meshwork. In: Smelser GK, ed. *The Structure of the Eye. New* York: Academic Press; 1961:335–341.
14. Svedbergh B. Protrusions of the inner wall of Schlemm's canal. *Am J Ophthalmol.* 1976;82:875–882.
15. Lee WR, Grierson I. Relationships between intraocular pressure and the morphology of the outflow apparatus. *Trans Ophthalmol Soc U K.* 1974;94:430–449.
16. Melamed S, Pei J, Epstein DL. Delayed response to argon laser trabeculoplasty in monkeys. *Arch Ophthalmol.* 1986;104:1078–1083.
17. Johnson DH. Histologic findings after argon laser trabeculoplasty in glaucomatous eyes. *Exp Eye Res.* 2007;85:557–562.
18. Honig MG, Hume RL. Fluorescent carbocyanine dyes allow living neurons of identified origin to be studied in long-term cultures. *J Cell Biol.* 1986;103:171–187.
19. Dvorak-Theobald G. Further studies on the canal of Schlemm: its anastomoses and anatomic relations. *Am J Ophthalmol.* 1955;39:65–89.
20. Selbach JM, Rohen JW, Steuhl KP, Lutjen-Drecoll E. Angioarchitecture and innervation of the primate anterior episclera. *Curr Eye Res.* 2005;30:337–344.
21. Johnson MC, Kamm RD. The role of Schlemm's canal in aqueous outflow from the human eye. *Invest Ophthalmol Vis Sci.* 1983;24:320–325.
22. Rohen JW, Futa R, Lutjen-Drecoll E. The fine structure of the cribriform meshwork in normal and glaucomatous eyes as seen in tangential sections. *Invest Ophthalmol Vis Sci.* 1981;21:574–585.
23. Scott PA, Overby DR, Freddo TF, Gong H. Comparative studies between species that do and do not exhibit the washout effect. *Exp Eye Res.* 2007;84:435–443.
24. Johnson M, Shapiro A, Ethier CR, Kamm RD. Modulation of outflow resistance by the pores of the inner wall endothelium. *Invest Ophthalmol Vis Sci.* 1992;33:1670–1675.
25. Neustadt J, Pieczenik S. Organ reserve and healthy aging. *Int Med.* 2008;7:50–52.